

Part I : Tilt sub-grain boundaries

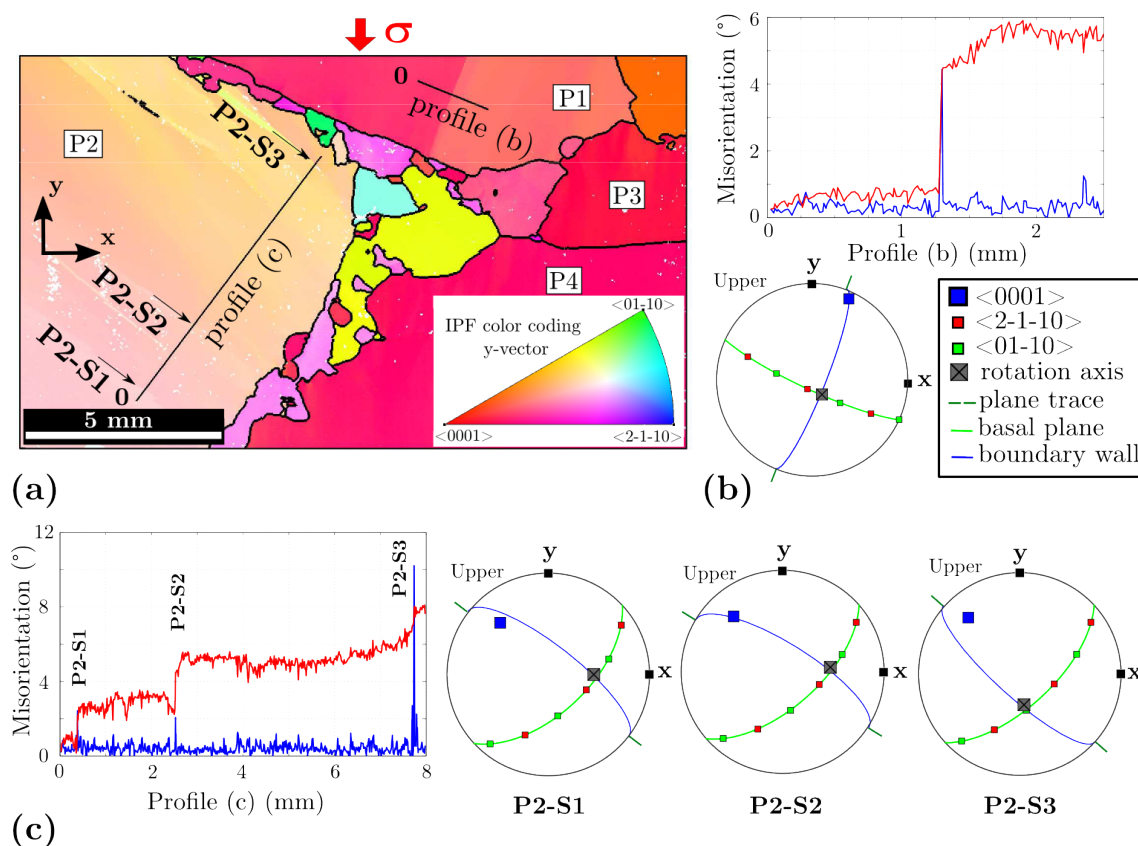
Tilt sub-grain boundaries (tilt SGB) are the most commonly observed substructures in the laboratory experiments presented in this study or in previous studies [1–3]. These boundaries have geometries consistent with a tilt wall of edge dislocations [4].

A well-defined tilt SGB is illustrated in Grain P1 in supplementary figure 1 (a). The misorientation profile 1 across this SGB (Fig. Supp 1 (b)) shows a sharp orientation gradient (below the EBSD step-size of 20 μm) with a misorientation higher than 4° between the two sides of the SGB. The pole figure (Fig. Supp 1 (b)) shows that the misorientation axis is between $\langle a \rangle$ and $\langle m \rangle$ direction in the basal plane and stands within the basal plane. In order to fully define this SGB as a tilt SGB, we need to make the assumption that the sub-grain wall is roughly perpendicular to the sample surface and not parallel to it (Fig. Supp 1 (b)). That is supported by geometrical probability which predicts a high probability for a 2D section to cut boundaries normal to the surface [14].

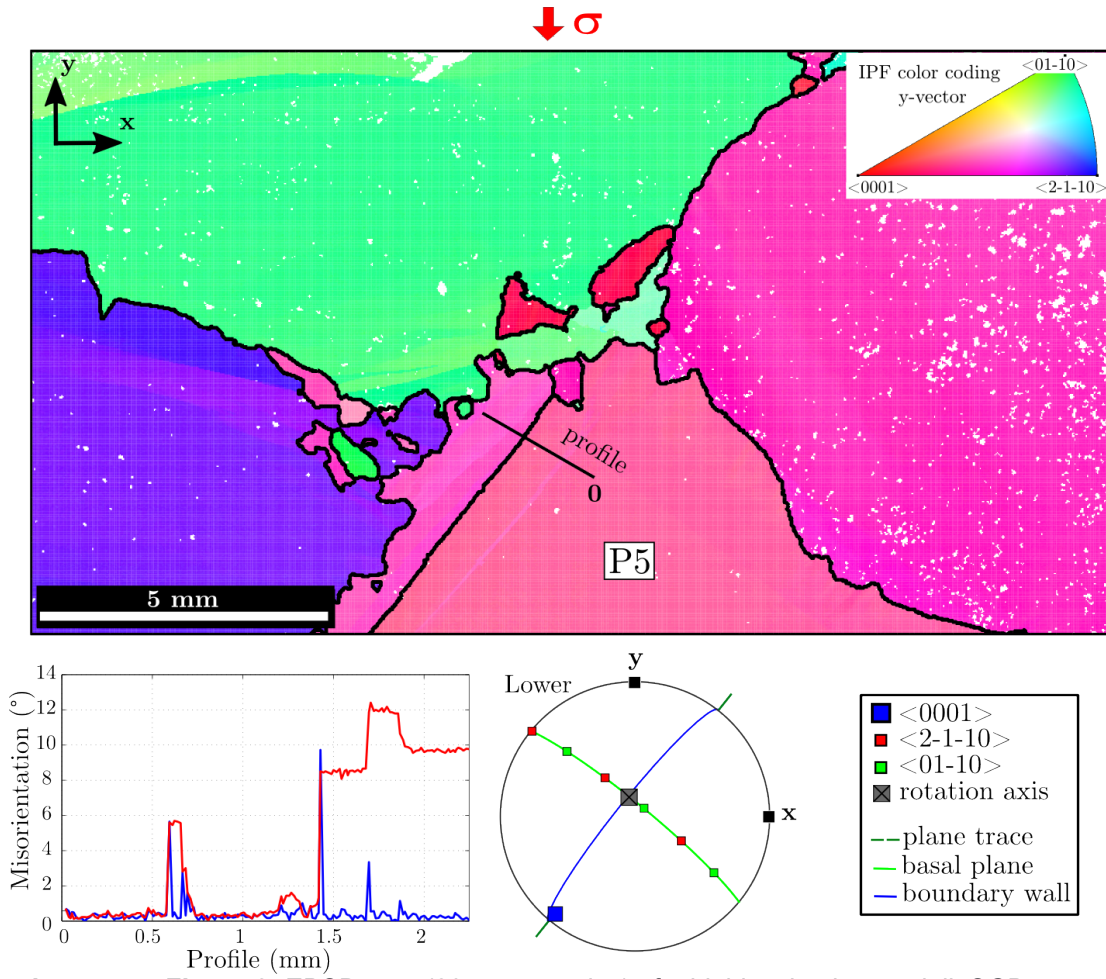
This assumption, already made by Piazzolo et al. [1] is reasonable given the columnar geometry of the sample, but only 3D measurements could confirm it. Based on this assumption and considering that the c-axis lies within the SGB plane, we can hypothesize that this tilt SGB is essentially composed by basal edge dislocations with $\langle a \rangle$ Burgers vectors.

A similar reasoning enables to distinguish similar tilt SGBs in grain P2 (Fig. Supp 1 (c)) and P5 (Fig. Supp 2). The misorientation profile across grain P2 and the pole figures showing the crystallographic orientation of the crystal and the misorientation axes highlight bending of the grain P2 by multiple tilt SGBs, which result in a cumulate misorientation up to 8° .

In grain P5, the misorientation profile (Fig. Supp 2, bottom) shows at least five SGBs identified as tilt SGBs. Those within 0.5 and 0.8 mm or 1.6 and 1.9 mm from the start of the profile are organized as kink bands made of two tilt SGBs with opposite misorientation axes. The SGB located at 1.4 mm from the start of the profile also has characteristics consistent with a tilt SGB, but cumulates a misorientation $> 8^\circ$. It could therefore be considered as a new grain boundary.



Supplementary Figure 1: (a) EBSD color map (20 μm step size). (b) Misorientation profile 1 and associated misorientation axis analysis for the sub-grain boundary from grain P1. (c) Misorientation profile 2 and associated misorientation axis analysis for the 3 sub-grain boundaries visible in grain P2 (S1, S2 and S3).



Supplementary Figure 2: EBSD map (20 μm step size) of a highly misorientated tilt SGB. Misorientation along the profile crossing the tilt sub-grain boundary is given at the bottom left, and pole figure showing the rotation axis is given at the bottom right.

Part II : Transition between sub-grain boundary and grain boundary

The transition between sub-grain boundary and grain boundary is not clearly defined in ice. Historically the segmentation performed on deep ice cores was done by looking to the grain shape through cross polarized light [5, 6]. Many studies talk about transition between sub-grain boundary and grain boundary and give no precise angle [7, 8]. Recent studies by Weikusat et al. [3] calculated a lower bound for the transition between tilt SGB and GB at around 5° for a tilt made of basal dislocations and 3° for a tilt made of non-basal dislocations. These values were obtained by estimating the SGB energy based on calculation that considers individual dislocations. Doing so, they underestimate the angle of transition between SGB and GB as they overestimate the SGB energy.

Read and Shockley [9] proposed a model to calculate the energy of a tilt “ γ ” made of edge dislocations, and creating a misorientation θ ranging between 0 and 15° :

$$\gamma = \gamma_0 * \theta * (A - \ln \theta) \quad (1)$$

$$A = 1 + \ln \left(\frac{b}{2\pi r_0} \right) \quad \gamma_0 = \frac{G * b}{4\pi(1 - \mu)} \quad (2)$$

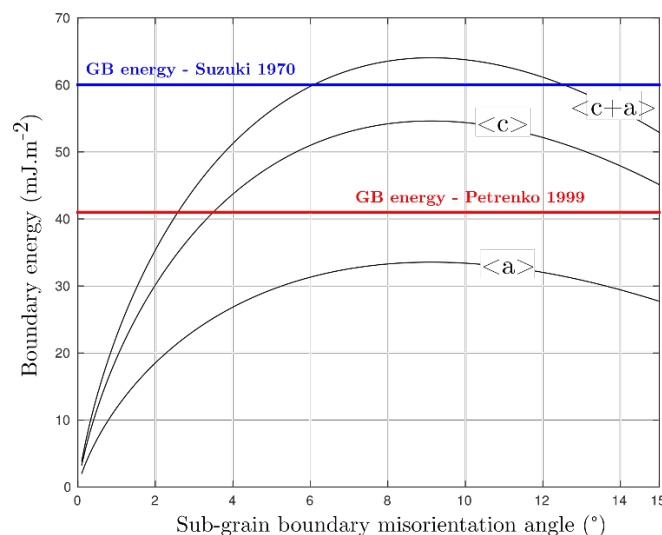
Where G is the shear modulus ($3.4 \times 10^9 \text{ N.m}^{-2}$), μ the Poisson's ratio (0.41) [10] and r_0 the dislocation core radius which is between b and $5b$ [11], with b the norm of the Burgers vector of the dislocations forming the SGB. The value of b depends on the dislocations involved within the tilt SGB considered. $b = 4.52 \text{ \AA}$ for a tilt SGB made of basal $\langle a \rangle$ dislocations, $b = 7.36 \text{ \AA}$ for a tilt SGB made of non-basal $\langle c \rangle$ dislocations and $b = 8.63 \text{ \AA}$ for $\langle c+a \rangle$ dislocations [12].

Existing measurements of grain boundary energy, based on grooving technique [10], provide a large range of values from 42 mJ.m^{-2} , as given in [10] to between 60 and 100 mJ.m^{-2} as found by [13].

Supplementary figure 3 shows the calculated tilt SGB energy by using the Read and Shockley [9] model, equation 1, with $r_0 = b$. We can see that the SGB energy decreases after 8° which is incoherent with the fact that more dislocations must be involved for higher misorientations. This provides the upper bound for the Read and Shockley [9] model in the case of ice.

Depending on the GB energy chosen from the literature, the energetically defined transition between sub-grain boundary and grain boundary varies. In particular, it depends on the type of dislocations creating the tilt SGB. The strong anisotropy of the ice single crystal makes it harder to clearly define this transition. For instance, a tilt SGB formed of basal $\langle a \rangle$ dislocations will remain energetically more favorable than a grain boundary whatever the misorientation created (and therefore the dislocation density), up to the limit of the model (around 8°).

Adding on top of that the fact that the model describes only tilt SGB and not twist SGB or mixed SGB, a transition between sub-grain boundary and grain boundary at 7° , such as selected in this study, appears coherent and is, at least, the best we can do.



Supplementary Figure 3: Sub-grain boundary energy calculated using the Read and Shockley [9] model for a tilt sub-grain boundary. The black curves show three configurations with different types of dislocations, $\langle a \rangle$, $\langle c \rangle$, and $\langle c+a \rangle$. The blue and red lines show different value of grain boundary energy proposed in the literature.

References

1. Piazzolo S, Montagnat M, Blackford JR. 2008 Sub-structure characterization of experimentally and naturally deformed ice using cryo-EBSD. *Journal of Microscopy* **230**, 509–519.
2. Montagnat M, Blackford JR, Piazzolo S, Arnaud L, Lebensohn RA. 2011 Measurements and full-field predictions of deformation heterogeneities in ice. *Earth and Planetary Science Letters* **305**, 153–160.
3. Weikusat I, Miyamoto A, Faria SH, Kipfstuhl S, Azuma N, Hondoh T. 2011 Subgrain boundaries in Antarctic ice quantified by X-ray Laue diffraction. *Journal of Glaciology* **57**, 111–120.
4. Friedel J. 1964 Dislocations. Oxford **70**, 15–24.
5. Duval P, Lorius C. 1980 Crystal size and climatic record down to the last ice age from Antarctic ice. *Earth and Planetary Science Letters* **48**, 59–64.
6. Jacka TH, Jun L. 1994. The steady-state crystal size of deforming ice. *Annals of Glaciology* **20**, 13–18.

7. Montagnat M, Durand G, Duval P. 2009 Recrystallization Processes in Granular Ice. *Low Temperature Science* **68**, 81–90.
8. Wilson CJ, Petermann M, Piazzolo S, Luzin V. 2013 Microstructure and fabric development in ice: Lessons learned from *in situ* experiments and implications for understanding rock evolution. *Journal of Structural Geology*.
9. Read WT, Shockley W. 1950 Dislocation Models of Crystal Grain Boundaries. *Physical Review* **78**, 275–289.
10. Petrenko VF, Whitworth RW. 1999 *Physics of Ice*. Clarendon Press.
11. Humphreys FJ, Hatherly M. 2004 *Recrystallization and Related Annealing Phenomena*, Second Edition. Pergamon, 2 edition.
12. Hondoh T. 2000 Nature and behavior of dislocations in ice. *Physics of ice core records* pp. 3–24.
13. Suzuki S. 1970 Grain coarsening of microcrystals of ice (III). *Low Temp. Sci., Ser. A* **28**, 47–61.
14. Kendall, M. G., and P. A. P. Moran. "Geometrical probability. Griffin's Statistical Monographs & Courses, No. 10." *London, England: Griffin* (1963).